Editors' Suggestion

Experimental evidence for the microscopic mechanism of the unusual spin-induced electric polarization in $GdMn_2O_5$

G. Yahia,[1,2] F. Damay,[3] S. Chattopadhyay,[4,5,*] V. Balédent,[1] W. Peng,[1] S. W. Kim,[6] M. Greenblatt,[6] M.-B. Lepetit,[7,8] and P. Foury-Leylekian[1]

[1]*Laboratoire de Physique des Solides, CNRS, Université Paris-Sud, Université Paris-Saclay, 91405 Orsay Cedex, France*

[2]*Laboratoire de Physique de la Matière Condensée, Université Tunis-El Manar, 2092 Tunis, Tunisia*

[3]*Laboratoire Léon Brillouin,CEA-CNRS UMR12, 91191 Gif-sur-Yvette Cedex, France*

[4]*Université Grenoble Alpes, INAC-MEM, F-38000 Grenoble, France*

[5]*CEA-Grenoble, INAC-MEM, F-38000 Grenoble, France*

[6]*Department of Chemistry and Chemical Biology, Rutgers, The State University of New Jersey, Piscataway, New Jersey 08854, USA*

[7]*Institut Néel, CNRS UPR 2940, 25 Avenue des Martyrs, 38042 Grenoble, France*

[8]*Institut Laue Langevin, 72 Avenue des Martyrs, 38042 Grenoble, France*

(Received 30 October 2017; revised manuscript received 17 January 2018; published 15 February 2018)

We report in this paper the temperature evolution of the magnetic structure of $GdMn_2O_5$, in the range 2–40 K, studied by neutron diffraction on an isotope-enriched powder. We detail a thorough analysis of the microscopic mechanisms needed to release the different magnetic frustrations that are at the origin of the polarization. In addition to the usual exchange-striction term, known to be at the origin of the polarization in this family, an additional exchange-striction effect between the Gd^{3+} and Mn^{3+} spins is found to be responsible for the very large polarization in the Gd compound.

DOI: 10.1103/PhysRevB.97.085128

Multiferroic materials, stabilizing at least two different but simultaneous orders, generally magnetism and ferroelectricity, are potentially useful materials for applications, owing to their versatility and multifunctionality [1]. For the technological development of magnetoelectric multiferroics, the optimization of performances such as the coupling between magnetic and ferroelectric orders is required. This optimization is, however, challenging, since most of the current magnetoelectric multiferroic materials present either a weak electric polarization or a weak magnetoelectric coupling.

Recently, a sizable magnetoelectric effect has been measured in several members of the RMn_2O_5 (R = rare earth) manganites [2]. $GdMn_2O_5$, for instance, presents an electric polarization of $\sim 3600\,\mu C/m^2$ [3–5], a value nearly able to compete with the so-called Bi manganite multiferroics [6]. In addition, its unusually strong electric polarization is also highly sensitive to applied magnetic fields [3]. The challenge is to understand the microscopic origin of this spin-induced ferroelectricity, and to pinpoint the specificity of Gd among other rare earths. In most of the spin-induced multiferroics, the Dzyaloshinskii-Moriya interaction between noncollinear spins has been proposed as the microscopic mechanism of the magnetic ferroelectricity. However, in the case of the RMn_2O_5 family, the observation of a perfectly collinear spin arrangement along the c axis in $SmMn_2O_5$ has recently definitively ascribed the ferroelectricity to an Mn-Mn exchange-striction model [7]. Gd-Mn symmetric exchange striction, in addition to the Mn-Mn exchange-striction mechanism, has recently been suggested in order to explain the large polarization measured in $GdMn_2O_5$ [3] but without any proposed microscopic mechanism. Moreover, the determination of the $GdMn_2O_5$ magnetic structure was done using resonant x-ray magnetic scattering, which provides no information on the moments' absolute value or their relative phases.

For a more accurate understanding of the origin of the unusually large polarization of $GdMn_2O_5$, a precise magnetic structure determination is required, ideally from neutron-scattering experiments. Owing to the extremely high neutron absorption of the Gd nucleus, such an experiment had never been attempted to date. We present in this paper the first powder neutron diffraction experiment performed on an isotope (^{160}Gd) enriched compound. From this measurement we deduce the magnetic structure as a function of the temperature. Furthermore, by a detailed analysis of the exchange terms, we show evidence of the microscopic mechanism responsible for the strong electric polarization in the Gd member.

The RMn_2O_5 compounds crystallize in the Pm space group [8]. Nevertheless, owing to the small distortions away from the average $Pbam$ structure, the latter will be used in the magnetic refinements which will follow. Along the c direction, the RMn_2O_5 structure is composed of chains of $Mn^{4+}O_6$ octahedra, separated by layers of R^{3+} or Mn^{3+} ions. In the (a,b) plane, zigzag chains of $Mn^{4+}O_6$ octahedra and $Mn^{3+}O_4$ pyramids run along the a axis, and are stacked along the b axis (see Fig. 1).

Along c, there are two relevant $Mn^{4+} - Mn^{4+}$ exchange interactions, J_1 (through the R^{3+} layers) and J_2 (through the Mn^{3+} layers) [9]. While J_2 is intrinsically antiferromagnetic, it is strongly frustrated by the $Mn^{4+} - Mn^{3+}$ interactions. This always results in a ferromagnetic ordering of the Mn^{4+} ions.

*Dresden High Magnetic Field Laboratory (HLD-EMFL), Helmholtz-Zentrum Dresden-Rossendorf, 01314 Dresden, Germany.

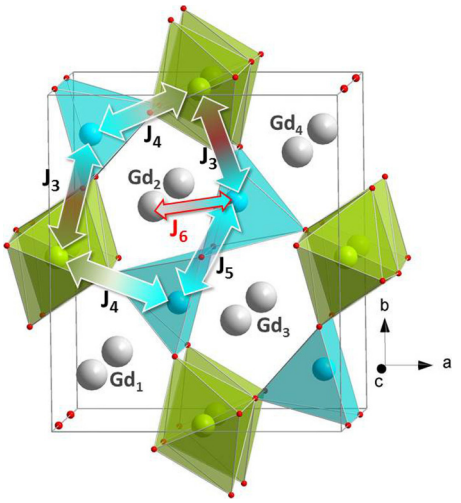

FIG. 1. Perspective view of the $R\mathrm{Mn_2O_5}$ crystal structure and relevant magnetic exchanges. The Mn^{4+} (green) ions are in an octahedral coordination shell and the Mn^{3+} (cyan) ions are in a square-based pyramidal coordination shell. Exchange terms J_i are detailed in the text.

The case of the J_1 interaction is more complex and leads to the various incommensurate magnetic orders observed in the $R\mathrm{Mn_2O_5}$ members when R is varied. The magnetic frustration inherent to this structure comes mostly from the exchange interactions in the (a,b) plane. There are three nonequivalent magnetic superexchange paths, J_3 and J_4, between Mn^{4+} and Mn^{3+} spins, and J_5 between two Mn^{3+} spins (Fig. 1). The main contribution to these exchanges is the antiferromagnetic (AF) Mn-Mn superexchange interaction through a shared oxygen. J_4 and J_5 are expected to be the dominant integrals [10], while J_3 is frustrated. The influence of the rare earth is generally neglected in the exchange Hamiltonian, owing to the strong spatial localization of their orbitals. However at low temperature and in the particular case of Gd^{3+} with its giant spin ($4f^7$ electronic configuration), the superexchange interaction between $Gd^{3+} - Mn^{3+}$ spins through a common oxygen (labeled J_6 in the following and on Fig. 1) can become relevant, as first proposed in Ref. [11]. The fingerprint of the importance of this J_6 interaction has recently been identified using inelastic neutron scattering in $\mathrm{DyMn_2O_5}$ [12]. Notice that another exchange interaction between Mn^{4+} and R^{3+} has been introduced by Zhao *et al.* [13] but is expected to be smaller than the one involving Mn^{3+} and can be shown to be irrelevant for the onset of the polarization.

Previous heat capacity measurements performed on $\mathrm{GdMn_2O_5}$ have evidenced a succession of three phase transitions, at $T_1 \simeq 38$ K, $T_2 \simeq 32$ K, and $T_3 \simeq 5$ K [14]. The low-temperature transition is not accurately defined because of the width of the heat capacity peak, which spreads from 10 to 2 K. Concomitantly with the T_2 transition, a sharp peak is observed in the real part of the dielectric constant, with a shoulder already present at T_1 [5]. Below a temperature close to T_3, another peak is observed in the dielectric constant measurement [15]. Furthermore, polarization measurements show that between T_1 and T_2, the b component of the polarization is minute and starts

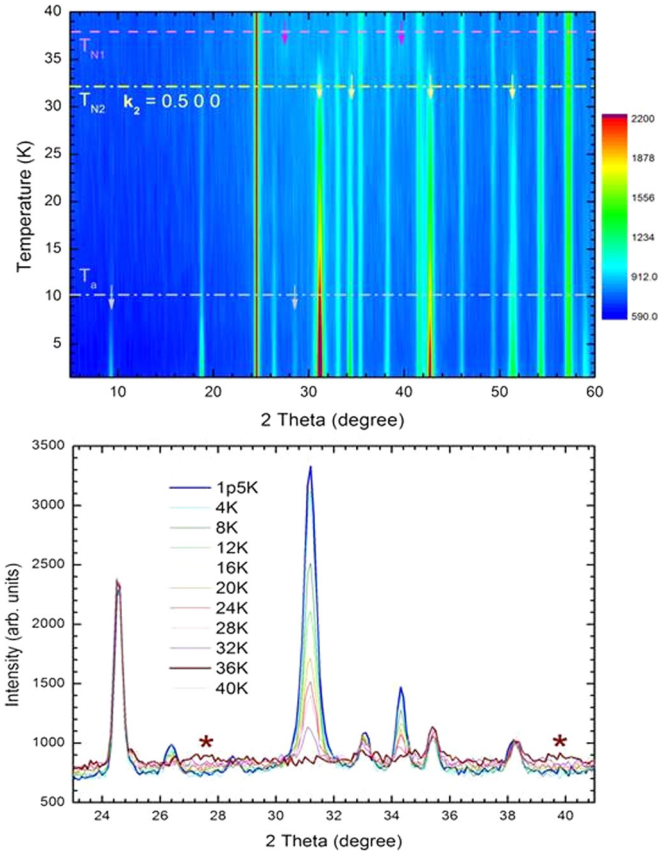

FIG. 2. Temperature evolution of the powder neutron diffraction patterns of $\mathrm{GdMn_2O_5}$ between 40 and 2 K. The bottom panel is a zoom on the main magnetic Bragg peak profile in the same temperature range. Stars correspond to the two magnetic peaks identified at 36 K in the incommensurate magnetic phase.

to really develop only below T_2. It slightly increases below 10 K but does not saturate down to 2 K.

The measurements presented in this paper were performed on a high-purity and high-quality powder, whose synthesis was carried out following the process described in Ref. [16], starting from a ^{160}Gd-enriched $\mathrm{Gd_2O_3}$ oxide.

Neutron powder diffraction experiments were carried out on a 1-g powder sample, on the G4.1 diffractometer (Orphée-LLB, CEA-Saclay, France). The neutron wavelength was 2.426 Å. Measurements were performed by heating up the sample from 2 to 40 K, with a step of 4 K above 4 K. Rietveld refinements of the crystal and magnetic structures were performed with the FULLPROF program [17], and symmetry analysis was performed using tools from the Bilbao crystallographic server (see Ref. [18] and references within).

The temperature evolution of the diffractograms is shown in Fig. 2. The results evidence three magnetic transitions at $T_1 = 40$ K, $T_2 = 32$ K, and $T_a = 12$ K. T_1 and T_2 coincide with the presence of the anomalies in the heat capacity and dielectric constant measurements, while at T_a, an anomaly in the temperature dependence of the electric polarization has been detected by various authors [3,19,20].

The propagation wave vector between T_1 and T_2 is of the type $\mathbf{q_{ICM}} = (0.5\text{-}\delta_1, 0, 0.2\text{-}\delta_2)$, compatible with the reported (0.49, 0, 0.18) [3]. Only two very weak and broad magnetic

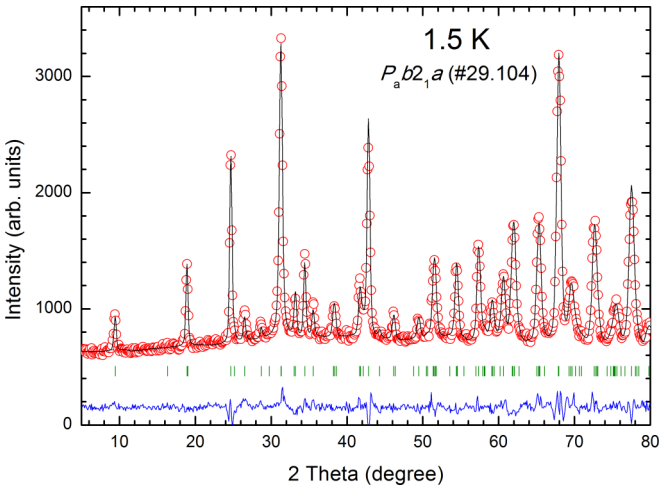

FIG. 3. Rietveld refinement of the neutron diffraction data of $GdMn_2O_5$ at 1.5 K. The experimental data are in red, the calculated profile in black, and their difference in blue. Green ticks indicate Bragg peak positions.

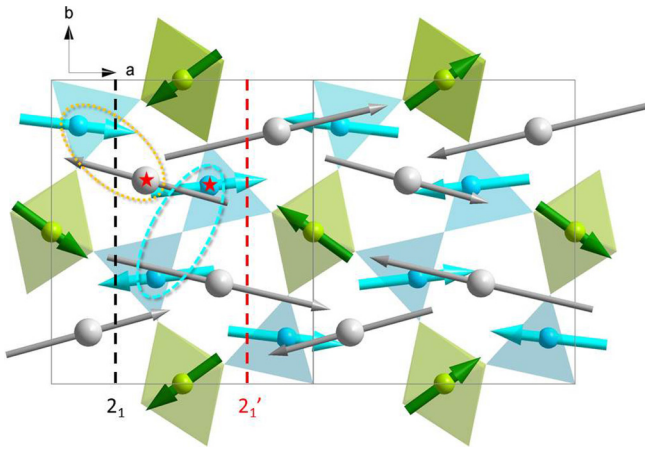

FIG. 4. Magnetic structure of $GdMn_2O_5$ at 1.5 K. The blue (orange) ellipses show the Mn^{3+}/Mn^{3+} (Gd^{3+}/Mn^{3+}) AF pairs. Stars identify the Gd/Mn^{3+} pair proposed by Lee *et al.* in their model [3].

Bragg peaks can be seen on the 36-K diffraction pattern (see bottom panel of Fig. 2), thus preventing any accurate description of the magnetic ordering in this temperature range. Below T_2, in contrast, several new magnetic Bragg reflections appear (Fig. 2). These reflections can be indexed with a commensurate magnetic propagation vector $\mathbf{q}_{CM} = (0.5, 0, 0)$. The magnetic intensity at low temperature is much stronger than generally observed in the other compounds of the series, indicating a strong magnetic contribution of the Gd^{3+} spins.

As the symmetry breaking from the $Pbam$ to Pm space group remains weak in the RMn_2O_5 family, the symmetry analysis was performed starting from the $Pbam\bar{1}$ paramagnetic group. There are four possible maximal subgroups compatible with a q_{CM} magnetic ordering. As reported [3], only $P_a ca2_1$ (or $P_a b2_1 a$ in the parent cell setting) provides a satisfactory refinement of the diffraction data. Note that it is also the only allowing a collinear arrangement of the Gd and Mn species spins, and a nonzero polarization tensor along b. In this magnetic space group, because of the loss of inversion symmetry, there are two pairs of Gd [(Gd1, Gd2) and (Gd3, Gd4), Fig. 1], which are independent. Within each pair, Gd spins are related by a 2_1 or a $2_1'$ rotation. There are two distinct Mn^{3+} pairs as well. In order to reduce the number of free parameters in the refinement, the magnitude of the moments for same species ions was initially set to be equal. Releasing the constraint on the Gd^{3+} moment amplitudes, however, leads to a substantial improvement of the refinement. The best Rietveld profile at 1.5 K is shown in Fig. 3 and the corresponding magnetic order in Fig. 4.

The results of the refinement show that at 1.5 K, all the moments lie in the (a,b) plane, with a systematically larger component along a than along b (see also Table I). The usual feature of $TbMn_2O_5$, that is, the antiferromagnetic ordering (due to J_5) between edge-sharing Mn^{3+} tetrahedra pairs (blue ellipse in Fig. 4), is also found in $GdMn_2O_5$. The antiparallel arrangement of specific Gd/Mn^{3+} pairs (orange ellipse in Fig. 4) is also striking, as it is not an imposed constraint. Mn^{4+} spins lie within the equatorial plane of their octahedral environment. The Gd moments are nearly fully ordered, between 5.5 μ_B for the (Gd1, Gd2) pair and 6.4 μ_B for the (Gd3, Gd4) pair, at 1.5 K. Mn^{3+} and Mn^{4+} moment values are comparable to those published for other members of the RMn_2O_5 series, with 3.3 and 2.6 μ_B, respectively, at 1.5 K. Note that the magnetic ordering proposed by Lee *et al.* [3] is almost in perfect agreement with the one determined here from neutron diffraction. The main difference is in the Gd/Mn antiparallel pairs, which couple in the x-ray model the closest Mn-Gd atoms (outlined by stars in Fig. 4). Another minor difference lies in the estimation of the ordered moment, which is in this study slightly higher for Gd and lower for Mn spins, as Lee *et al.* had to assume that Mn spins were saturated at their spin-only expected value, which is not quite the case, according to our results.

It is possible, with increasing temperature, to use the same model to refine the diffraction data. However, above 12 K, the disappearance of two reflections, namely, (100) and (300), allows one to propose a model of the magnetic structure where all spins are aligned along a, without deteriorating the refinement (see Fig. 5). Although this is not a definite proof that the magnetic structure is actually collinear, it would explain the anomaly seen around 12 K, as the temperature at which spins depart from collinearity. The evolution of the ordered moment with temperature is shown in Fig. 6 and does not depend (within the error bars) on the model chosen to refine the data. Two interesting conclusions can be made from this evolution: first, that Gd moments order as early as 32 K, as was already intuited by several authors [3], and

TABLE I. Magnetic structure parameters of $GdMn_2O_5$ at 1.5 K in the $P_a b2_1 a$ cell (i.e., doubled along a).

	x/a	y/b	z/c	M_x	M_y	$M_{tot}(\mu_B)$
Mn^{3+}	0.199	0.348	0.5	–3.3(1)	–0.4(1)	3.3(1)
Mn^{4+}	0	0.5	0.252	2.2(1)	–1.4(1)	2.6(1)
Gd1	0.07	0.169	0	5.4(1)	0.9(1)	5.5(1)
Gd3	0.923	0.831	0	–6.3(1)	–1.3(1)	6.4(1)

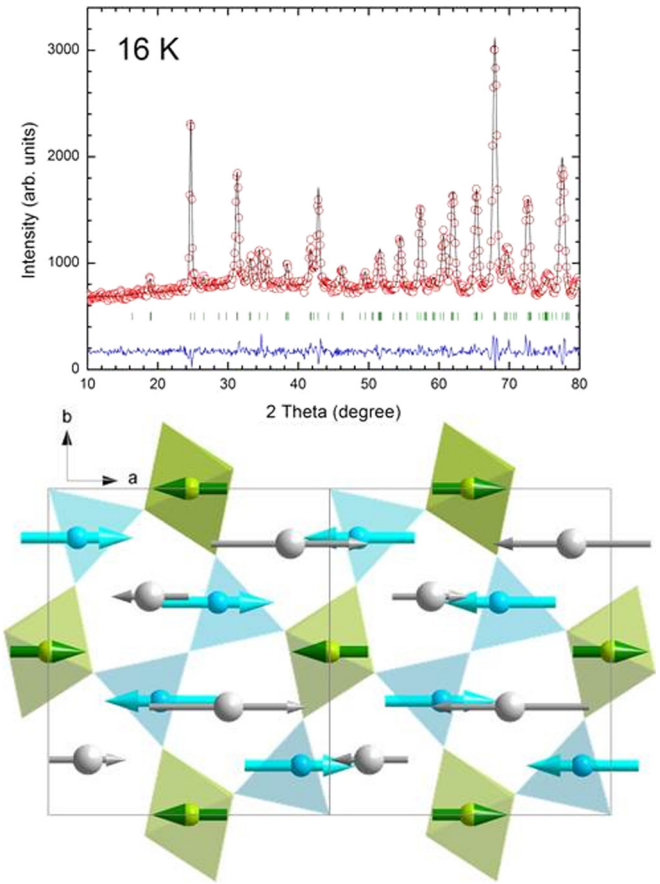

FIG. 5. Rietveld refinement and corresponding magnetic structure of $GdMn_2O_5$ at 16 K.

second, from the shape of the Gd moment vs T curve, that Gd moments do order in the effective magnetic field created by the Mn spins ordering. We applied the molecular-field model in order to calculate these thermal variations. The temperature

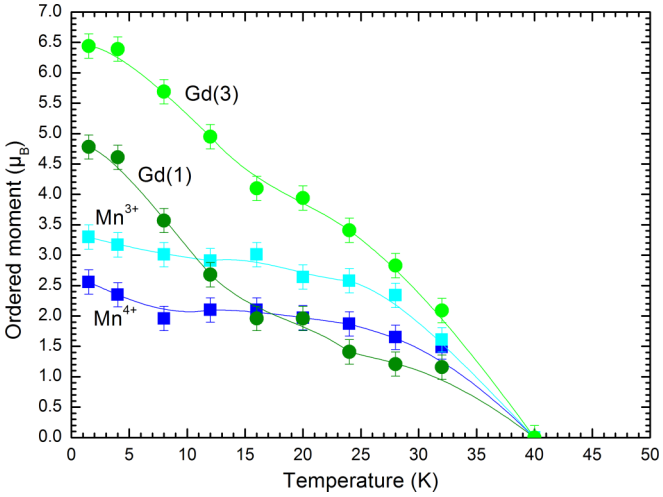

FIG. 6. Temperature evolution of the magnetic moments on the Mn^{4+}, Mn^{3+}, and Gd^{3+} sites in $GdMn_2O_5$ (from Rietveld refinements of neutron diffraction data, assuming a collinear magnetic structure above 16 K).

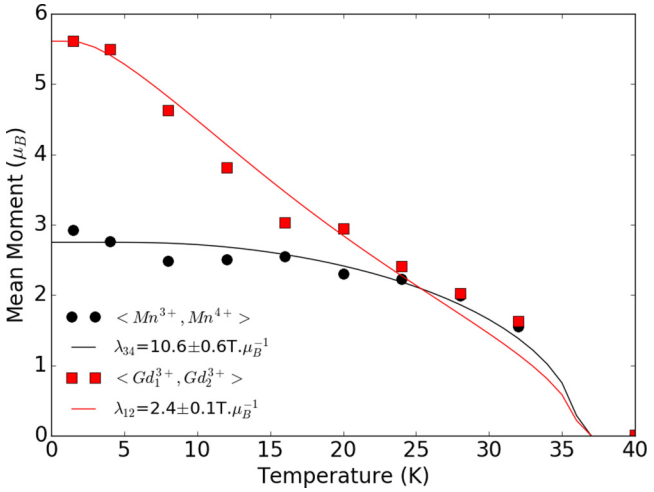

FIG. 7. Temperature dependence of mean Mn (black circles) and Gd (red squares) moments. Lines correspond to the self-consistent mean-field calculation fit for Mn and Gd in the molecular field of the mean Mn moments.

dependence of the Mn mean moments is determined by the usual self-consistent mean-field calculation [21], giving a coupling $\lambda_0 = 10.6 \pm 0.6T\mu_B^{-1}$. A similar fit for the mean moments of the two Gd in the molecular field of the mean Mn moments gives a coupling value of $\lambda_1 = 2.4 \pm 0.1T\mu_B^{-1}$ (see Fig. 7). The coupling between Gd and Mn is then 4 times smaller than that of the coupling between Mn and Mn. The main contributions to Mn-Mn coupling come from J_4 and J_5 ($\sim$2.9 meV and 3.5 meV in $TbMn_2O_5$ [10]), since J_1 and J_2 are an order of magnitude smaller ($\sim$0.4 meV in $TbMn_2O_5$ [10]) and J_3 fully compensated within the $Pbam$ mean space group and thus not contributing. We can then expect the coupling between Mn and Gd (related to an effective J_6) to be one-fourth that of J_4 and J_5, and thus around 0.7 meV.

At this point let us redo the magnetic symmetry analysis from a quantum mechanical point of view. One should first remember that in quantum mechanics the symmetry of a system is not related to the space-time operators leaving its ground state (or its magnetic part) invariant (as assumed in magnetic diffraction), but that the magnetic space group is the set of space-time symmetry operators leaving the Hamiltonian of the system invariant. In the Born-Oppenheimer approximation (fixed, classical nuclei), it means the set of operators leaving the electrostatic potential generated by the nuclei and the spin-orbit operators invariant. Group theory then tells us that the ground-state wave function Ψ, and thus its magnetic part, must belong to one of the irreducible corepresentations Γ_n of the magnetic group $\mathcal{G}$ but not necessarily to the totally symmetric Γ_1 one. In other words, one must have : $\forall \hat{g} \in \mathcal{G}, \hat{g}\Psi = \lambda_g \Psi$ with $\lambda_g \in \mathbb{C}$, but not necessarily $\forall \hat{g} \in \mathcal{G}, \lambda_g = 1$, characteristic of the Γ_1 irreducible representation. Diffraction data tells us that the crystallographic group for the RMn_2O_5 family is Pm [8]. It is easy to show that the magnetic group is $\mathcal{G}$: Pm' (see Supplemental Material [22]). At the X point (1/2 0 0) of the Brillouin zone, the Pm' group has two irreducible corepresentations, X_1 and X_2. According to group theory, states belonging to X_1 are symmetric with respect to m', while

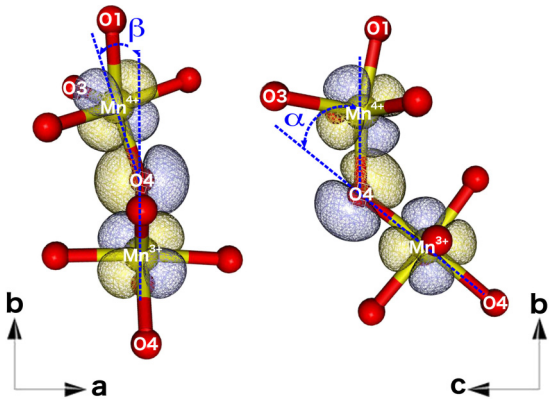

FIG. 8. Superexchange paths for the J_3 magnetic exchange (see Fig. 1) in the (a, b) and (b, c) planes. With this angle convention, $J_3 \simeq J_{\pi\pi}\cos\beta + J_{\pi\pi}\cos\alpha$.

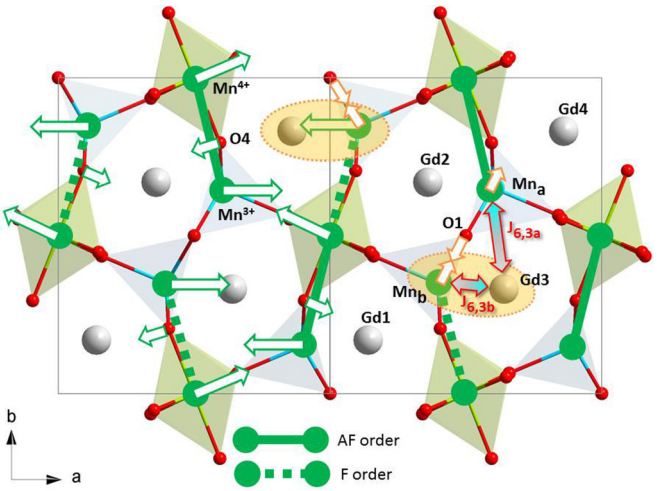

FIG. 9. Atomic displacements associated with the release the magnetic frustration at the origin of the polarization. On the left half of the unit cell, displacements represented by green arrows are due to the exchange-striction mechanism involving J_3 (Fig. 8). On the right half, gold arrows stand for displacements due to the additional exchange-striction mechanism involving J_6. Gold ellipses englobe the Gd-Mn^{3+} coupled by J_6 via O_1. The global displacement is along $+\vec{b}$ direction for Mn ions and along $(-\vec{b})$ for O, resulting in a polarization along b.

states belonging to X_2 are asymmetric. Applied to the magnetic moments of the Mn and Gd ions, this means the following:

Within X_1: Each of the Gd^{3+}, Mn^{3+}, and Mn^{4+} within the unit cell are independent, the Gd^{3+} and Mn^{3+} moments must be in the (a,b) plane, while there are no conditions on the orientation of the Mn^{4+} moments;

Within X_2: Each of the Gd^{3+}, Mn^{3+}, and Mn^{4+} within the unit cell are independent, the Gd^{3+} and Mn^{3+} moments must be along c, while there are no conditions on the orientation of the Mn^{4+} moments.

One sees immediately that the magnetic structure found for the $GdMn_2O_5$ compound thus belongs to the X_1 irreducible representation of the magnetic Pm' group.

In the framework of the exchange-striction mechanism (ES), we can precisely describe the mechanism at the origin of the electric polarization created by the magnetic order in $GdMn_2O_5$ and more generally in the RMn_2O_5 compounds. Let us recall that the magnetic frustration within the Mn pentagons is directly related to the J_3 magnetic exchanges (Fig. 1). Indeed, in the $Pbam$ nonpolar group, J_3 does not contribute to the magnetic energy as its two contributions cancel out: in each unit cell one is located between atoms with a FM ordering while the other is between atoms with an antiferromagnetic (AFM) ordering (see Figs. 4 or 5). It is thus the symmetry breaking from $Pbam$ to Pm which allows the two J_3 interactions to be inequivalent, that is, responsible for the observed polarization. Indeed, to release the magnetic frustration, one needs atomic displacements increasing the J_3 superexchange term between antiferromagnetically ordered moments and decreasing it between ferromagnetically ordered ones [7]. Following the analysis of Ref. [10], the main way to modify J_3 is to change the angles α and β in order to maximize the $Mn^{3+}(t_{2g})$–$O_4(2p)$–$Mn^{4+}(t_{2g})$ orbitals' overlap (see Fig. 8). Increasing the AFM character of J_3 thus means decreasing α and β towards 0. As a consequence, the Mn^{3+} ions will shift alternatively along the $\pm a$ direction, the Mn^{4+} along the $\pm a + \varepsilon b$, while the O_4 oxygen bridging the Mn^{3+} and Mn^{4+} ions will move alternatively along the $\pm a - \eta b$ direction (see Fig. 9). Within the entire unit cell these shifts result in a global relative displacement of the negative charges along $-b$ and of the positive ones along the $+b$ direction, i.e., in a macroscopic electric polarization along b and a symmetry breaking of the inversion center.

To further understand the unusually high value of the polarization in the specific case of $GdMn_2O_5$, let us now analyze the Gd–Mn interactions. One should first remember that the Gd^{3+} ion is in a $4f^7$, $S = 7/2$, $L = 0$ configuration. As a result, in a first approximation (spherical, atomic), the spin-orbit interactions on the Gd^{3+} ground state and thus the Gd^{3+} magnetic anisotropy are nill. Another consequence is a distance-only dependence of some of the factors involved in J_6. Using the quasidegenerate perturbation theory [23] on an effective Hubbard model based on the $4f$ orbitals of the Gd, the $3d$ orbitals of the Mn, and the $2p$ orbitals of the bridging oxygens, one can write the Gd–Mn superexchange terms from the fourth order in the usual way (see, for instance, [24], [25] and related references),

$$J_6 \simeq -\sum_{2p}\sum_{i}(t_{f,p})^2\,(t_{p,d_i})^2\left(\frac{2}{(\Delta E_f)^2 U_f}+\frac{2}{(\Delta\, E_d)^2 U_d}\right), \tag{1}$$

where $t_{f,p}$ is the transfer integral between the set of $4f$ orbitals of the Gd ion and the $2p$ orbitals of the bridging oxygen, t_{p,d_i} is the transfer integral between the occupied $3d_i$ orbital of the Mn ion and the bridging oxygen $2p$ orbital, ΔE_f is the ligand-to-Gd charge-transfer energy and ΔE_d the ligand-to-Mn charge-transfer energy, and finally, U_f and U_d are the repulsion integrals of a double occupation in the Gd $4f$ and Mn $3d$ shells, respectively. Due to the $4f^7$ configuration of the Gd^{3+} ion, the Gd-O factors in J_6 depend only on the Gd-O distance. As a result, the strongest J_6 interactions should be the ones bridged by the oxygen closest to the Gd. At low temperature this is the O_1 (Fig. 9) oxygen, which also mediates

the strongest Mn–Mn interaction J_5. In fact, as can be seen in Figs. 4 and 9, O_1 mediates the interaction between the Mn^{3+} dimer and two Gd ions, namely, Gd_2 and Gd_3 (see Fig. 9), resulting in a strong magnetic frustration. Let us investigate, within the framework of a Heisenberg Hamiltonian in mean-field approximation, whether exchange striction can induce additional atomic displacements that release this frustration. One can model the local magnetic energy as

$$E = J_{6,2a}\langle\vec{S}_{Gd_2}\rangle\cdot\langle\vec{S}_{Mn_a^{3+}}\rangle + J_{6,2b}\langle\vec{S}_{Gd_2}\rangle\cdot\langle\vec{S}_{Mn_b^{3+}}\rangle + J_{6,3a}\langle\vec{S}_{Gd_3}\rangle\cdot\langle\vec{S}_{Mn_a^{3+}}\rangle + J_{6,3b}\langle\vec{S}_{Gd_3}\rangle\cdot\langle\vec{S}_{Mn_b^{3+}}\rangle.$$

In a *Pbam* structural group, one would have

$$J = J_{6,2a} = J_{6,3a} = J_{6,2b} = J_{6,3b},$$
$$\vec{s} = \langle\vec{S}_{Mn_a^{3+}}\rangle = -\langle\vec{S}_{Mn_b^{3+}}\rangle,$$
$$\vec{S} = -\langle\vec{S}_{Gd_2}\rangle = \langle\vec{S}_{Gd_3}\rangle,$$

with $J_{6,ia}$ the exchange term between Gd_i and Mn_a (see Fig. 9), resulting in $E = 0$. In a subgroup compatible with the disproportionation of all the Gd moments as observed in the 1.5-K magnetic structure one has

$$\vec{S}_2 = \langle\vec{S}_{Gd_2}\rangle \neq \vec{S}_3 = -\langle\vec{S}_{Gd_3}\rangle \quad \text{and} \quad S_2 < S_3,$$

and thus $E = J[\vec{S}_2\cdot(\vec{s}-\vec{s}) + \vec{S}_3\cdot(\vec{s}-\vec{s})] = 0$. In order to release the magnetic frustration and lower E one therefore needs further action, such as, for instance, atomic displacements. Indeed, a movement increasing the amplitude of the J_6 interaction coupling the largest AFM Gd_3-Mn_b interaction [as S(Gd3) > S(Gd1)] should lower the magnetic energy, as can be seen in the following equations:

$$J_a = J_{6,2a} = J_{6,3a} \neq J_b = J_{6,2b} = J_{6,3b} \quad \text{and} \quad |J_a| < |J_b|,$$
$$\vec{S}_2 = \langle\vec{S}_{Gd_2}\rangle \neq \vec{S}_3 = -\langle\vec{S}_{Gd_3}\rangle \quad \text{and} \quad S_2 < S_3,$$

that yield

$$E = (J_a - J_b)\,(\vec{S}_3 - \vec{S}_2)\cdot\vec{s} \quad < \quad 0.$$

As can be seen from Eq. (1), such atomic displacements must increase the $(t_{p,d_i})^2$ factors and thus the overlap between the oxygen $2p$ orbitals and the Mn_b^{3+} 3d ones. Indeed, as the Mn-Gd magnetic exchanges are mediated by the oxygens [see Eq. (1)], a displacement of the Gd ions will result in an equal modification of $J_{6,2b}$ and $J_{6,3b}$ (similarly $J_{6,2a}$ and $J_{6,3a}$) and thus will not lift the frustration. This means that one must shorten the $O_1-Mn_b^{3+}$ bond and lengthen the $O_1-Mn_a^{3+}$ bond, as pictured on the right part of Fig. 9. These displacements do not interfere with the original exchange striction, issued from the release of the J_3 frustration. They result in a further increase of the polarization along b, responsible for the very large value of the $GdMn_2O_5$ polarization among the RMn_2O_5 family.

The possibility of an additional mechanism has been previously proposed but neither experimentally demonstrated nor discussed in detail until now [3,19]. At 12 K the structural data exhibit a crossover between the $Gd-O_1$ and $Gd-O_2$ distances, the $Gd-O_2$ becoming the shortest. In contrast to the O_1 oxygen, the O_2 ions do not mediate any magnetic frustration and thus at $T > 12$ K, the frustration weakens and thus the extra polar displacements.

In conclusion, we report the first powder neutron diffraction on an isotope-enriched compound of $GdMn_2O_5$. The refined magnetic structure in the commensurate and ferroelectric phase shows a comparable magnetic structure to most of the other members of the RMn_2O_5 series: spins in the (a,b) plane. In the context of the exchange-striction mechanism, we show in this paper that not only the release of the frustration related to the $Mn^{3+}-Mn^{4+}$ J_3 interaction is at play, but an additional exchange-striction effect, releasing the J_6 frustration between the huge and isotropic Gd^{3+} moments and the Mn^{3+} spins, is responsible for a large extra term in the polarization. These findings suggest that the isotropic character and thus the spin-orbit coupling may play a crucial role in the polarization amplitude yet to be confirmed. As a conclusion, one may foresee that the complete and accurate understanding of the role of the rare earth in the multiferroic properties of this series of compounds paves the way to exploratory research on spin-induced multiferroic materials where the choice of rare earth will be a tool to improve the performances.

This work was supported by project CMCU PHC UTIQUE 15G1306. The work of M. Greenblatt was supported by NSF-DMR Grant No. 1507252. This work was also supported by the Chinese Scholarship Council.

[1] W. Eerenstein, N. D. Mathur, and J. F. Scott, Nature (London) **442**, 759 (2006).
[2] N. Hur, S. Park, P. Sharma, J. S. Ahn, S. Guha, and S.-W. Cheong, Nature (London) **429**, 392 (2004).
[3] N. Lee, C. Vecchini, Y. J. Choi, L. C. Chapon, A. Bombardi, P. G. Radaelli, and S.-W. Cheong, Phys. Rev. Lett. **110**, 137203 (2013).
[4] A. Inomata and K. Kohn, J. Phys.: Condens. Matter **8**, 2673 (1996).
[5] B. Khannanov, E. I. Golovenchits, and V. A. Sanina, J. Phys.: Conf. Series **572**, 012046 (2014).
[6] D. Lebeugle, D. Colson, A. Forget, and M. Viret, Appl. Phys. Lett. **91**, 022907 (2007).
[7] G. Yahia, F. Damay, S. Chattopadhyay, V. Balédent, W. Peng, E. Elkaim, M. Whitaker, M. Greenblatt, M.-B. Lepetit, and P. Foury-Leylekian, Phys. Rev. B **95**, 184112 (2017).
[8] V. Balédent, S. Chattopadhyay, P. Fertey, M. B. Lepetit, M. Greenblatt, B. Wanklyn, F. O. Saouma, J. I. Jang, and P. Foury-Leylekian, Phys. Rev. Lett. **114**, 117601 (2015).
[9] P. G. Radaelli and L. C. Chapon, J. Phys.: Condens. Matter **20**, 434213 (2008).
[10] S. Petit, V. Balédent, C. Doubrovsky, M. B. Lepetit, M. Greenblatt, B. Wanklyn, and P. Foury-Leylekian, Phys. Rev. B **87**, 140301 (2013).

[11] Y. F. Popov, A. M. Kadomtseva, G. P. Vorob'ev, S. S. Krotov, K. I. Kamilov, and M. M. Lukina, Phys. Solid State **45**, 2155 (2003).
[12] S. Chattopadhyay, S. Petit, E. Ressouche, S. Raymond, V. Balédent, G. Yahia, W. Peng, J. Robert, M.-B. Lepetit, M. Greenblatt, and P. Foury-Leylekian, Sci. Rep. **7**, 14506 (2017).
[13] Z. Y. Zhao, M. F. Liu, X. Li, L. Lin, Z. B. Yan, S. Dong, and J. M. Liu, Sci. Rep. **4**, 3984 (2014).
[14] M. Tachibana, K. Akiyama, H. Kawaji, and T. Atake, Phys. Rev. B **72**, 224425 (2005).
[15] E. Golovenchits and V. Sanina, J. Phys.: Condens. Matter **16**, 4325 (2004).
[16] C. Doubrovsky, G. André, A. Gukasov, P. Auban-Senzier, C. R. Pasquier, E. Elkaim, M. Li, M. Greenblatt, F. Damay, and P. Foury-Leylekian, Phys. Rev. B **86**, 174417 (2012).
[17] J. Rodriguez-carvajal, Physica B (Amsterdam) **192**, 55 (1993).
[18] F. Damay, J. Phys. D: Appl. Phys. **48**, 504005 (2015).
[19] L. H. Yin, D. H. Jang, C. B. Park, K. W. Shin, and K. H. Kim, J. Appl. Phys. **119**, 104101 (2016). .
[20] C. Lu, J. Fan, H. Liu, K. Xia, K. Wang, P. Wang, Q. He, D. Yu, and J.-M. Liu, Appl. Phys. A **96**, 991 (2009).
[21] X. Fabrèges, I. Mirebeau, P. Bonville, S. Petit, G. Lebras-Jasmin, A. Forget, G. André, and S. Pailhès, Phys. Rev. B **78**, 214422 (2008).
[22] See Supplemental Material at http://link.aps.org/supplemental/10.1103/PhysRevB.97.085128 for spin-orbit and mirror operators matrices within 4*f* shells.
[23] I. Lindgren and J. Morrison, *Atomic Many- Body Theory* (Springer-Verlag, New York, 1982).
[24] N. Suaud and M.-B. Lepetit, Phys. Rev. B **62**, 402 (2000).
[25] A. Gellé and M.-B. Lepetit, Phys. Rev. B **74**, 235115 (2006).